2011 50th IEEE Conference on Decision and Control and
European Control Conference (CDC-ECC)
Orlando, FL, USA, December 12-15, 2011

Bounded Control of an Actuated Lower Limb Orthosis

Hala Rifaï, Walid Hassani, Samer Mohammed and Yacine Amirat

Abstract— **Wearable robots have defined a new horizon for elderly and disabled people, to regain control of their limbs, as well as for healthy people, to increase their abilities of hard missions execution. The present paper deals with the control of a lower limb orthosis applied at the knee joint level for rehabilitation purposes. A bounded control torque is developed in order to guarantee the asymptotic stability of the knee orthosis. The control law respects the physical constraints of the system. Moreover, it is robust with respect to external disturbances. The effectiveness of the control torque is tested in real-time using the EICOSI orthosis of the LISSI Lab.**

I. Introduction

Wearable robots are anthropomorphic, mechatronic systems that fit the geometry of the human body and work in harmony with it. These robots collect signals from the embodying limbs, by means of on-board sensors, and transfer adaptable power to the limbs allowing to move them by means of actuators. Defined trajectories of the limbs can then be executed by applying adequate controls to the embodied actuator. Note that wearable robots are intended for two main applications: the increase of the wearer's performance in terms of energy economics, joint strength and endurance specially for load transfer purposes [1], [2] and the assistance of people suffering from physical weakness in order to help them regaining control of their limbs (rehabilitation and assistance of paralyzed persons and elderly).

Different works have dealt with the control of exoskeletons having multiple degrees of freedom. The control in [2] is based on a scaled compensation of the estimated exoskeleton dynamics. Proportional derivative (PD) feedback is widely used to control the exoskeletons. In [3], the control torque is a proportional one at the hip level, proportional to the square of the angular velocity at the knee joint level, and the whole cycle of walking is ensured using a state machine aiming to increase the load carrying. Exoskeletons are also used for gait rehabilitation. For example, a PD coupled to a constant-value control, balancing the gravity when the foot is on the ground, is applied to control the leg's trajectory of a paraplegic patient and/or stabilize its body in [4]. A PD with gravity, friction and coriolis forces compensation and a force field controller are developed in [5] for stroke patients. A fictitious gain is introduced in [6] to balance the change in body's dynamics during walking, load, etc. and tested with a proportional-integrator-derivative controller (PID). A fuzzy control is developed in [7] and a neural networks based control in [8] aiming to assist human walking. However, none of these works has proved the exoskeleton's stability.

Exoskeletons or orthoses having only one degree of freedom, at the knee or ankle levels, have also been developed especially for gait rehabilitation. In the following, only the works concerning the control of the knee are presented. Some works have proposed to assist people through affording a part of the effort necessary to achieve a movement, allowing to relax their muscles. The desired movement is computed by measuring EMG signals in [9] to achieve sit-to-stand movements and climbing stairs, and by measuring the ground reaction force in [10] to enhance the endurance. The controller in this case acts as an amplifier. Note that no desired trajectories are defined and therefore no position controller is used. Another approach consists on modifying the impedance parameters of the human limbs by setting those of the embodied exoskeleton. This strategy allows to increase the leg's natural frequency and facilitates its flexion and extension movements consequently. It is achieved in [11] by modifying the damping parameter with respect to the motion intention, used to compute the desired orientation which is tracked by means of PID controller. The exoskeleton and user's inertia compensation is considered in [12] using a positive feedback of low pass-filtered knee's angular acceleration to determine a desired shank orientation that is tracked by means of a Linear Quadratic (LQ) controller. In the last two works, the shank embodying the exoskeleton is modeled as a mass, spring, damper, sparing all system's non-linearities. Note that none of the aforecited works has considered the physical constraints of the system.

The paper deals with the control of the EICOSI (Exoskeleton Intelligently COmmunicating and Sensitive to Intention) having one degree of freedom at the knee level. It is intended to be used for rehabilitation purposes by people having knee joint impairments. The EICOSI orthosis is not cumbersome and easy to don and doff which makes it very practical to use by knee-joint disabled persons. The proposed control torque ensures the asymptotic stability of the orthosis/wearer for flexion-extension movements. Note that the stance phase of locomotion has not been taken into account. The control is bounded in order to take into account the provided power limitation as well as the saturation of the actuator and prevent consequently problems related to nonlinearities. As a first approach, the wearer is considered completely passive, only rehabilitation movements are studied and, the totality of the gravity torque is compensated.

This work lies within the scope of project EICOSI (Exoskeleton Intelligently COmmunicating and Sensitive to Intention), sponsored by the regional council of Ile-De-France.

H. Rifaï, W. Hassani, S. Mohammed and Y. Amirat are with the Laboratory of Images, Signals and Intelligent Systems (LISSI), EA 3956, University of Paris-Est Créteil, IUT Créteil-Vitry, Dept. R&T, 122 Rue Paul Armangot, 94400 Vitry-Sur-Seine, France. E-mails: {hala.rifai, samer.mohammed, amirat}@u-pec.fr, walid1.hassani@etu.u-pec.fr

The paper is structured as follows. The orthosis model as well as its parameters identification are presented in section II. The bounded control torque is proposed in section III and the system's stability is proved. Real-time experimentations are addressed in section IV. Finally, conclusions are presented in section V and future works are introduced.

II. Shank-Orthosis Model and Parameters Identification

The system considered in the present work includes the orthosis as well as the wearer leg. Movements of flexions and extensions of the leg will be studied in a seated position of the wearer for purposes of rehabilitation.

A. Shank-Orthosis Modeling

As mentioned previously, the design of the orthosis should match the body's geometry. In the project EICOSI, the orthosis is one structure having two segments related along a rotational axis. The first segment embodies the thigh while the second embodies the shank and are fixed to the wearer by means of braces (Fig. 1 and 3). The orthosis should be fixed to the human leg such that they have the same rotational degree of freedom at the knee level. As a sequel, the orthosis and the leg are assumed coupled.

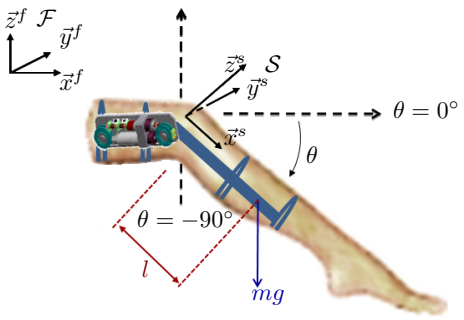

Fig. 1. Human leg embodying the orthosis: Fixed and Shank frames.

Denote by $\mathcal{F}(\vec{x}^f, \vec{y}^f, \vec{z}^f)$ a fixed frame in the space and by $\mathcal{S}(\vec{x}^s, \vec{y}^s, \vec{z}^s)$ a frame attached to the shank at the knee defined such that the direction of $\vec{y}^f$ and $\vec{y}^s$ coincide (Fig. 1). The knee, and therefore the orthosis, are in rotation about the pitch axis $\vec{y}^s$ of an angle θ. Since the system has only one degree of freedom, its angular velocity is equal to the derivative of the rotational position. Let θ and $\dot{\theta}$ denote the angular position and velocity of the shank relative to the thigh, respectively. In the following, the model of the shank-orthosis movement is given. The shank and orthosis models will be derived similarly. The kinetic and gravitational energies of the system are given by: $E_k = \frac{1}{2}J\dot{\theta}^2$ and $E_g = mgl(1 - \sin\theta)$, with J the inertia of the system in $\mathcal{S}$, m its mass, l the distance from the knee to the system's center of gravity and g is the gravity acceleration. Deriving the system's Lagrangian $\mathcal{L} = E_k - E_g$, the dynamics of the shank can be written as:

$$J\ddot{\theta} + mgl\cos\theta = \tau_{ext},$$

with τ_{ext} is the external torque acting on the system. It includes the friction torque τ_f and the control torque τ. The solid and viscous frictions are the main components of the friction torque. It is modeled as [13]:

$$\tau_f = -A\text{sign}\dot{\theta} - B\dot{\theta},$$

where A and B are the coefficients of solid and viscous friction torques respectively, sign$(\cdot)$ is the classical sign function. The main advantage of this model is the linearity in parameters A and B which facilitates their identification.

1) Shank's model: The wearer is considered completely passive. This has been monitored, during the experiments, by means of EMG electrodes used to detect and reject any muscular activity generated by the shank muscles. Therefore, the wearer is not developing any control torque. The model of the shank can then be written as:

$$J_s\ddot{\theta} + m_s g l_s \cos\theta = -A_s\text{sign}\dot{\theta} - B_s\dot{\theta}, \quad (1)$$

with J_s, m_s, l_s, A_s, B_s are respectively the inertia, mass, distance to the center of gravity, solid and viscous friction coefficients of the shank.

2) Orthosis' model: The orthosis' actuator delivers the whole power to drive the system. Therefore, the model of the orthosis can be written as:

$$J_o\ddot{\theta} + m_o g l_o \cos\theta = -A_o\text{sign}\dot{\theta} - B_o\dot{\theta} + \tau, \quad (2)$$

with J_o, m_o, l_o, A_o, B_o are respectively the inertia, mass, distance to the center of gravity, solid and viscous friction coefficients of the orthosis.

Summing (1) and (2), the system's (orthosis and shank) dynamics can therefore be written as:

$$J\ddot{\theta} = -\tau_g\cos\theta - A\text{sign}\dot{\theta} - B\dot{\theta} + \tau, \quad (3)$$

with $J = J_s + J_o$ the system's inertia, $\tau_g = (m_s l_s + m_o l_o)g$ the system's gravity torque in full extension position of the thigh, $A = A_s + A_o$ the system's solid friction coefficient, $B = B_s + B_o$ the system's viscous coefficient and τ the control torque applied by the actuator to drive the orthosis and consequently the shank to a desired orientation.

B. Parameters identification

The shank's and orthosis' parameters are identified separately using the weighted least square method.

1) Shank's parameters: The mass of the shank m_s and the position of its center of gravity l_s are determined based on [14] given the height and weight of the subject, which is a method commonly used in biomechanics. The other parameters are identified using the pendulum test. It consists on dropping the shank from a full extension position, letting it swing till the rest position (see (c) and (a) of Fig. 3). The angle θ is measured using the goniometer SG150 of Biometrics Ltd., attached to the leg at the knee level, such that its local frame coincides with the shank frame $\mathcal{S}$. The angular velocity and acceleration, $\dot{\theta}$ and $\ddot{\theta}$, are derived numerically. (1) is used to identify J_s, A_s and B_s, knowing the gravitational torque $m_s g l_s$, θ, $\dot{\theta}$ and $\ddot{\theta}$.

2) Orthosis' parameters: To identify the orthosis' parameters, an excitation sequence describing the trajectory of the angle θ is predefined as well as the angular velocity and acceleration, $\dot{\theta}$ and $\ddot{\theta}$ [15]. The desired trajectory of the shank, considered during the identification phase, is given by: $\theta(t) = \sum_{i=1}^{n} \frac{a_l}{\omega_f l} \sin(\omega_f l t) - \frac{b_l}{\omega_f l} \cos(\omega_f l t) + \theta_0$, with ω_f is the fundamental radian frequency of the Fourier series, $\frac{a_l}{\omega_f l}$ and $\frac{b_l}{\omega_f l}$ are the amplitudes of the sine and cosine functions, t is the time and θ_0 is the initial value of the trajectory. The torque developed by the actuator when subject to the excitation trajectory is computed using measurements of a current sensor. J_o, $m_o g l_o$, A_o and B_o can be identified using (2) and knowing τ, θ, $\dot{\theta}$ and $\ddot{\theta}$.

(1) and (2) can be written in the general form:

$$\Gamma_i = W_i(\theta, \dot{\theta}, \ddot{\theta})X + \rho_i,$$

where X is the vector of positive parameters to identify, $X \in \mathbb{R}^m$ with m the vector's dimension, Γ_i is the measured/computed torque during identification process, $W_i(\theta, \dot{\theta}, \ddot{\theta})$ is the observation vector and ρ_i is the residue representing measurement noise and modeling error, $i \in \{1, \ldots, n\}$ and n is the number of samples considered within the trajectory and the torques values. Note that $\Gamma = [\Gamma_1 \ldots \Gamma_n]^T \in \mathbb{R}^n$, $W = [W_1 \ldots W_n]^T \in \mathbb{R}^{n \times m}$ and $\rho = [\rho_1 \ldots \rho_n]^T \in \mathbb{R}^n$. The parameters vector $\hat{X} \in \mathbb{R}^m$ is then estimated using the least square optimization:

$$\hat{X} = \text{Arg min } \|\rho\|^2 = W^+ \Gamma,$$

with $W^+ \in \mathbb{R}^{m \times n}$ the pseudo-inverse of matrix W given by $W^+ = (W^T W)^{-1} W^T$. Note that ρ is considered as a vector of white noise having a null mean vector.
The optimization is performed using the following conditions: $-\frac{\pi}{2} rad \leq \theta \leq 0\, rad$, $-2.1\, rad/s \leq \dot{\theta} \leq 2.1\, rad/s$ and $-\pi\, rad/s^2 \leq \ddot{\theta} \leq \pi\, rad/s^2$.

III. Exoskeleton Control

A robust control should be applied to the orthosis in order to guarantee a fair trajectory tracking of the actuated orthosis. This control law takes into consideration two criteria related principally to the safety of the mechanism since it is in direct relation with the human body. Quick variations of the friction, induced by unpredictable movements and causing wear loading of the actuator, engender unacceptable behavior of the orthosis and, therefore is not balanced in the control law. On the other hand, a high value of the control torque necessitates high power to ensure it, which cannot be achieved in wearable robots because it affects the safety of the wearer. Besides, the saturation of the actuators can lead to undesirable closed loop behaviors resulting in robot's instability. Consequently, the actuator amplitude limitation is taken into consideration in the design of the control torque in order to avoid irreversible damages.
Bounded control has been treated in the literature for systems falling in the framework of integrators chains [16], [17], [18], [19], [20], rigid bodies [21] and manipulators [22], [23]. Note that the last case of applications is of interest in the present work because the orthosis falls within this category. The aforecited control laws of manipulators are mainly based on saturated PD/PID or composed of the sum of the saturations applied individually to proportional and derivative terms. In the present work, a control torque based on nested saturations is proposed allowing not only to maintain bounded inputs, but also to have a better management of the velocity and position convergence. The control law is simple and therefore adaptable for real-time applications like orthosis. Moreover, it ensures the asymptotic stability of the system.

Let's first define a saturation function $\text{sat}_N(x)$, bounded between $\pm N$, as:

$$\text{sat}_N(x) = \min(N, \max(-N, x)), \quad \forall x \in \mathbb{R} \tag{4}$$

The control torque and stability analysis are presented:

Proposition 1: Consider the knee-joint human-orthosis model described by (3) with θ and $\dot{\theta}$ the knee joint angle and angular velocity, respectively. Denote θ_d the desired orientation and $\tilde{\theta} = \theta - \theta_d$ the orientation error. The control torque bounded between $\pm\bar{\tau}$ and defined by:

$$\tau = -\text{sat}_{N_1}[k_1 \dot{\theta} + \text{sat}_{N_2}(k_2 \tilde{\theta})] + \tau_g \cos\theta, \tag{5}$$

asymptotically stabilizes (3) at $(\theta, \dot{\theta}) = (\theta_d, 0)$ with a domain of attraction equal to $[-\theta_{max}, 0] \times \mathbb{R}$. k_1 and k_2 are positive scalar parameters and $\text{sat}_{N_i}(\cdot)$, $i \in \{1, 2\}$, are saturation functions defined in (4) with N_i the saturation bounds chosen such that $N_1 > 2N_2 > 2A$. The saturation bound of the control torque is $\bar{\tau} = N_1 + \tau_g$.

Proof: Consider firstly that $k_2|\tilde{\theta}| > N_2$ and $k_1|\dot{\theta}| > N_1 - N_2 > N_2$.
Consider the Lyapunov function V positive definite and radially unbounded:

$$V = \frac{1}{2} J \dot{\theta}^2.$$

Based on the system's model (3) and the control torque (5), the derivative of the Lyapunov function V is given by:

$$\dot{V} = -B\dot{\theta}^2 - A\dot{\theta}\text{sign}\dot{\theta} - \dot{\theta}\text{sat}_{N_1}[k_1\dot{\theta} + \text{sat}_{N_2}(k_2\tilde{\theta})].$$

Since $|k_1\dot{\theta}| > N_2$, then $|k_1\dot{\theta} + \text{sat}_{N_2}(k_2\tilde{\theta})| > 0$. Therefore, $\dot{\theta}$ and $k_1\dot{\theta} + \text{sat}_{N_2}(k_2\tilde{\theta})$ are of the same sign. The Lyapunov function becomes:

$$\dot{V} = -B\dot{\theta}^2 - A\dot{\theta}\text{sign}\dot{\theta} - |\dot{\theta}|N_1.$$

The Lyapunov function V is decreasing and $|\dot{\theta}|$ consequently. $\dot{\theta}$ enters the set $\Omega_1 : \{\dot{\theta}, \tilde{\theta} : k_1|\dot{\theta}| < N_1 - N_2, k_2|\tilde{\theta}| > N_2\}$. In Ω_1, $k_1|\dot{\theta}| + N_2 < N_1$. $\text{sat}_{N_1}(\cdot)$ operates then in the linear region and the control torque (5) becomes:

$$\tau = -k_1\dot{\theta} - \text{sat}_{N_2}(k_2\tilde{\theta}) + \tau_g \cos\theta. \tag{6}$$

In Ω_1, define the Lyapunov function W as:

$$W = \frac{1}{2} J(\dot{\theta} + \lambda\tilde{\theta})^2 + \tilde{\theta}\text{sat}_{N_2}(k_2\tilde{\theta}) + \frac{1}{2}\lambda(B + k_1 - J\lambda)\tilde{\theta}^2,$$

with $0 < \lambda < \frac{B+k_1}{J}$ and $\kappa = N_2 - A > 0$.
The derivative of the Lyapunov function within the trajectories of the system is given by:

$$\begin{aligned}\dot{W} &= (\dot{\theta} + \lambda\tilde{\theta})[-(B + k_1 - J\lambda)\dot{\theta} - A\text{sign}\dot{\theta} \\ &\quad -\text{sat}_{N_2}(k_2\tilde{\theta})] + \dot{\theta}\text{sat}_{N_2}(k_2\tilde{\theta}) \\ &\quad +\tilde{\theta}\dot{\theta}\frac{d}{d\tilde{\theta}}(\text{sat}_{N_2}(k_2\tilde{\theta})) + \lambda(B + k_1 - J\lambda)\tilde{\theta}\dot{\theta}.\end{aligned}$$

Since $k_2|\tilde{\theta}| > N_2$ then $|\text{sat}_{N_2}(k_2\tilde{\theta})| = N_2$ and $\frac{d}{d\tilde{\theta}}(\text{sat}_{N_2}(k_2\tilde{\theta})) = 0$. The derivative of W becomes:

$$\begin{aligned}\dot{W} &= -(B + k_1 - J\lambda)\dot{\theta}^2 - A\dot{\theta}\text{sign}\dot{\theta} - \lambda\tilde{\theta}\text{sat}_{N_2}(k_2\tilde{\theta}) \\ &\quad -A\lambda\tilde{\theta}\text{sign}\dot{\theta}, \\ &\leq -(B + k_1 - J\lambda)\dot{\theta}^2 - A\dot{\theta}\text{sign}\dot{\theta} - \lambda|\tilde{\theta}|\kappa.\end{aligned}$$

W is then decreasing. $\dot{\theta}$, $\tilde{\theta}$ enter the set Ω_2 defined by $\Omega_2 : \{\dot{\theta}, \tilde{\theta} : k_1|\dot{\theta}| < N_1 - N_2, k_1|\tilde{\theta}| < N_2\}$. In Ω_2, $\text{sat}_{N_2}(\cdot)$ operates in the linear region and the control torque (6) becomes:

$$\tau = -k_1\dot{\theta} - k_2\tilde{\theta} + \tau_g \cos\theta. \tag{7}$$

Define in Ω_2 the Lyapunov function L as:

$$L = \frac{1}{2}J\dot{\theta}^2 + \frac{1}{2}k_2\tilde{\theta}^2.$$

Replacing (7) in (3), the derivative of L is given by:

$$\dot{L} = -(B + k_1)\dot{\theta}^2 - A\dot{\theta}\text{sign}\dot{\theta} \leq 0. \tag{8}$$

The Lyapunov function L is then decreasing till the angular velocity reaches the origin $\dot{\theta} \equiv 0$. In order to complete the proof, the LaSalle Invariance Principle is invoked. All the trajectories converge to the largest invariant set $\bar{\Omega}_3$ in $\Omega_3 = \{(\tilde{\theta}, \dot{\theta}) : \dot{L} = 0\} = \{(\tilde{\theta}, \dot{\theta}) : \dot{\theta} = 0\}$. To remain in this set, one must ensure that $J\ddot{\theta} = -k_2\tilde{\theta} = 0$ with $k_2 > 0$. Therefore, to remain in the set $\bar{\Omega}_3$, one should satisfy $\tilde{\theta} = 0$ which means that $\theta = \theta_d$. Therefore, $(\theta, \dot{\theta}) = (\theta_d, 0)$ is an asymptotically stable point of the closed-loop system with a domain of attraction equal to $[-\theta_{max}, 0] \times \mathbb{R}$. ■

IV. Experimentation and Robustness tests

The control law is tested in real-time using the EICOSI orthosis of the LISSI-Laboratory, University of Paris-Est Créteil (UPEC). The mechanical structure of the orthosis consists of two segments attached to the thigh and shank respectively by means of braces, with a rotation axis at the knee level. The orthosis is actuated using a brushless DC motor (BLDC) chosen because it delivers a relatively high torque and runs smoothly at low speeds. The maximal torque that can be delivered by the actuator is $\bar{\tau} = 13\,N \cdot m$. The orthosis is also equipped with an incremental encoder that measures the angle of the shank segment relative to the thigh one. The control torque is computed using a controller board (dSPACE-DS1103) equipped with an IBM processor running at $400\,Mhz$. The controller takes the measurement of the angle delivered by the EICOSI's sensor and the angular velocity obtained by a simple derivation as well as the desired angle and velocity. The controller board delivers the pulse width modulation (PWM) level to control the actuator's velocity. The control loop runs at $1\,kHz$, fixed due to current and position sensors constraints.
The block diagram is presented in Fig. 2.

Parameter	Value±s.d. (%)
Inertia (J_o)	$0.0117 \pm 3.5238\,Kg \cdot m^2$
Solid friction coefficient (A_o)	$0.3525 \pm 0.2491\,N \cdot m$
Viscous friction coefficient (B_o)	$0.6928 \pm 0.3811\,N \cdot m \cdot s \cdot rad^{-1}$
Gravity torque (τ_{g_o})	$0.2424 \pm 0.5518\,N \cdot m$

TABLE I
ORTHOSIS PARAMETERS IDENTIFICATION

Parameter	Value±s.d. (%)
Inertia (J_s)	$0.3883 \pm 0.8088\,Kg \cdot m^2$
Solid friction coefficient (A_s)	$0.2475 \pm 2.5782\,N \cdot m$
Viscous friction coefficient (B_s)	$0.3072 \pm 2.8567\,N \cdot m \cdot s \cdot rad^{-1}$
Gravity torque (τ_{g_s})	$4.7576\,N \cdot m$

TABLE II
SHANK PARAMETERS IDENTIFICATION

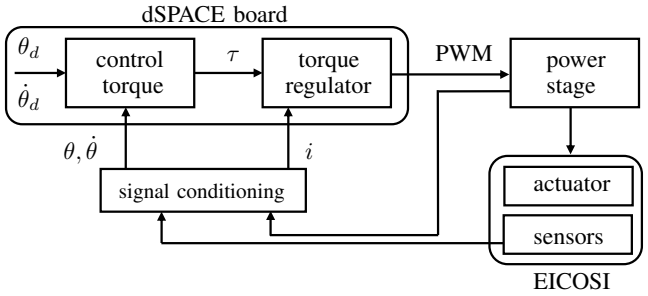

Fig. 2. Block diagram of the actuated orthosis in closed loop

The experiments are conducted on a healthy subject being 27 years old, weighing $90\,Kg$ and measuring $1.87\,m$. The parameters identification of the subject and the orthosis are described in section II. The system's (shank and orthosis) identified parameters: inertia, solid and viscous coefficients, the gravity torque are given in Tables I and II.

The saturation bounds of the control torque defined in (5) are set such that it respects the limitation of the supplied power and the maximal torque delivered by the actuator. Therefore, $N_1 = 8$ and $N_2 = \frac{8}{2.1}$. The control parameters are determined by poles placement at low velocities during the linear regime, they are set to: $k_1 = 20$ and $k_2 = 75$.

Two experiments are performed to test the efficiency of the control law. The first considers flexions and extensions of the knee, actions that are often achieved in rehabilitation phases. The desired trajectory is defined by successive steps functions. The control torque (5) is applied. Fig. 3 shows snapshots of the system's (shank + orthosis) trajectory. The angle, angular velocity and control torque are plotted in Fig. 4. Experiments show a good convergence of the angle at adaptable time. The control torque remains within the

(a) (b) (c)

Fig. 3. Successive positions of the shank during flexion-extension: (a) shows the rest position, (b) presents the shank during extension and (c) shows the full extension position.

saturation bounds avoiding the nonlinearities of the actuator. The angular velocity is not high, avoiding the wearer to endure high velocities that may be harmful for disabled people. When the shank reaches the desired position, the angular velocity is null and the control torque balances the shank and orthosis' weight. If the desired position is the full extension defined by angle $\theta = 0\,deg$, the control torque has the value of τ_g. The second experiment considers

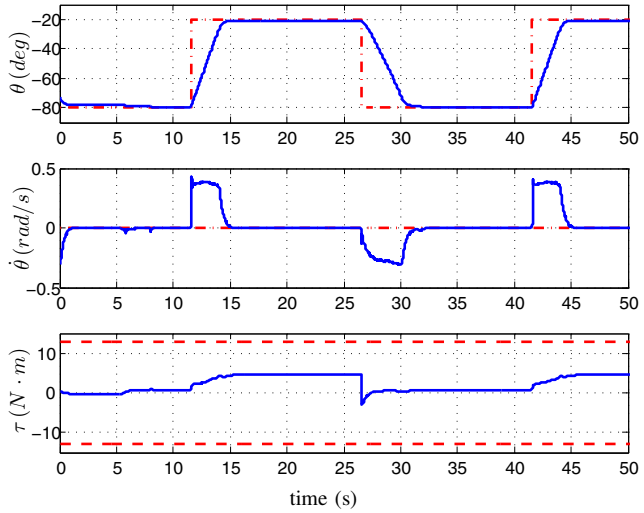

Fig. 4. Flexions and extensions: The knee-joint angle, angular velocity and control torque. The current values are plotted in continuous blue, the desired values in dot-dashed red, and the torque saturation bound in dashed red line.

a path tracking during locomotion phase of a person. A sinusoidal reference trajectory is considered. Control torque (5) is applied on the dynamics errors. The angle, angular velocity and control torque are presented in Fig. 5. The experiments show a good tracking of the angle and angular velocity, besides acceptable values of angular velocity and torque, which guarantees the safety of the wearer.

A. Robustness with respect to parameters identification

The control law is independent of the system's inertia, solid and viscous friction coefficients. However, the saturation bound of the scaled orientation error should always satisfy $N_2 > A$ to guarantee stability, condition that is maintained true since the solid friction coefficient has always a small value relative to the chosen bound N_2. The control depends only on the gravity torque. A bad estimation of this parameter does not induce instability. It would only create a

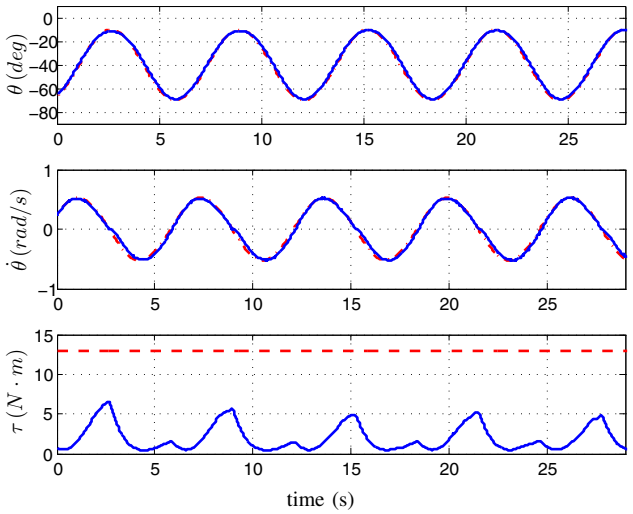

Fig. 5. Sinusoidal trajectory: The knee-joint angle, angular velocity and control torque. The current values are plotted in continuous blue, the desired values in dot-dashed red, and the torque saturation bound in dashed red line.

static error, *i.e.* the shank does not follow exactly the desired trajectory. Note that, during tests, τ_g can be adjusted in the control law to fit perfectly the wearer. This can be achieved technically using a simple potentiometer.

B. Robustness with respect to external disturbances

A misstep can be caused by a wrong movement at the knee level, it can cause instability or even falling down. Therefore, one main property of the control law is to regain the intended position whenever an unpredictable flexion occurs. In other words, the control law should be robust to external disturbances that may affect the knee and consequently the whole stability and safety of the wearer. The experiments consist on blocking the shank for a short period to highlight the robustness of the control law. The results are presented in Fig. 6 and 7 in both cases: flexion/extension and sinusoidal trajectory, respectively. In the first case, the control torque reaches the saturation bound before regaining stability. The saturation helps limiting the current used by the actuator to develop the desired torque and avoids its saturation. In the second case, the disturbance effect is almost not noticeable on the system's trajectory. In both cases, the angular velocities remain acceptable for the user.

V. Conclusions and Future Works

The present paper treated the control of a knee-joint orthosis. For this purpose, a model of the shank and orthosis has been proposed and its parameters have been identified using the weighted least-square method. A bounded control torque based on nested saturations with a gravity compensation has been proposed and its asymptotic stability has been proved using Lyapunov analysis. The control is low cost in terms of computation, independent of the system's inertia and friction model. Moreover, it is robust with respect to external disturbances allowing to guarantee the stability of the wearer in case of a wrong movement at the knee

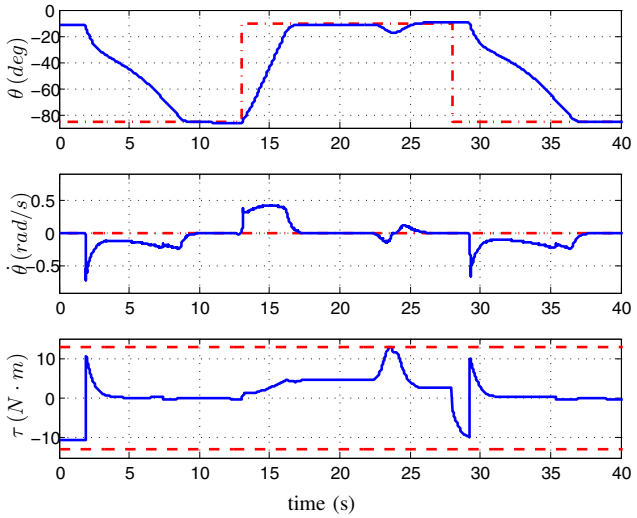

Fig. 6. Flexions and extensions in presence of external disturbances at $t = 22\,s$: The knee-joint angle, angular velocity and control torque. The current values are plotted in continuous blue, the desired values in dot-dashed red, and the torque saturation bound in dashed red line.

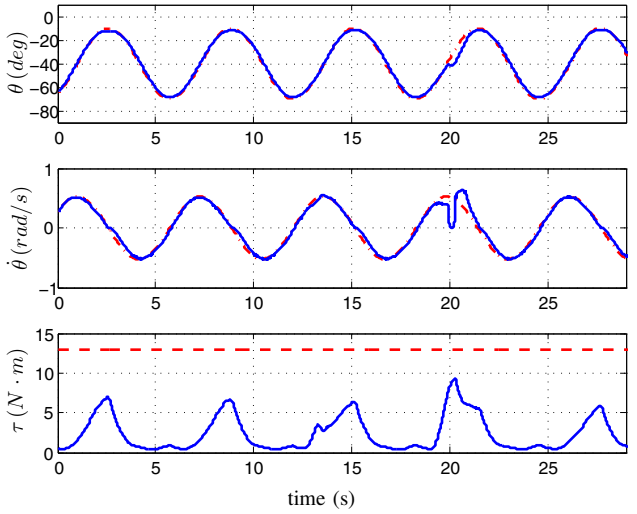

Fig. 7. Sinusoidal trajectory in presence of external disturbances at $t = 19\,s$: The knee-joint angle, angular velocity and control torque. The current values are plotted in continuous blue, the desired values in dot-dashed red, and the torque saturation bound in dashed red line.

level. The proposed control has been tested in real-time using the EICOSI orthosis of the LISSI Lab. Note that this work considers a completely passive wearer. Future works will integrate the contribution of the wearer by means of its muscles' effort, measured by EMG electrodes. The development of an exoskeleton to control more degrees of freedom of the lower limbs is also envisaged.

References

[1] H. Satoh, T. Kawabata, and Y. Sankai, "Bathing care assistance with robot suit HAL," in *Proceedings of International Conference on Robotics and Biomimetics*, China, 2009, pp. 498–503.

[2] H. Kazerooni, J.-L. Racine, L. Huang, and R. Steger, "On the control of the Berkeley lower extremity exeskeleton (BLEEX)," in *Porceedings of the International Conference on Robotics and Automation*, Barcelona, Spain, 2005, pp. 4364–4371.

[3] C.-J. Walsh, K.-P. Pasch, and H. Herr, "An autonomous, underactuated exoskeleton for load carrying augmentation," in *Proceedings of International Conference on Intelligent Robots and Systems*, Beijing, China, 2006, pp. 1410–1415.

[4] A. Tsukahara, R. Kawanishi, Y. Hasegawa, and Y. Sankai, "Sit-to-stand and stand-to-sit transfer support for complete paraplegic patients with robot suit HAL," *Journal of Advanced Robotics*, vol. 24, no. 1, pp. 1615–1638, 2010.

[5] S.-K. Banala, A. Kulpe, and S.-K. Agrawal, "A powered leg orthosis for gait rehabilitation of motor-impaired patients," in *Porceedings of the International Conference on Robotics and Automation*, Roma, Italy, 2007, pp. 4140–4145.

[6] K. Kong and M. Tomizuka, "Control of exoskeletons inpeired by fictitious gain in human model," *IEEE/ASME Transactions on Mechatronics*, vol. 14, no. 6, pp. 689–698, 2009.

[7] K. Kong and D. Jeon, "Design and control of an exeskeleton for the elderly and patients," *IEEE/ASME Transactions on Mechatronics*, vol. 11, no. 4, pp. 428–432, 2006.

[8] C.-J. Yang, B. Niu, and Y. Chen, "Adaptive neuro-fuzzy control based development of a wearable exoskeleton leg fo human walking power augmentation," in *Proceedings of International Conference on Advanced Intelligent Mechatronics*, CA, USA, 2005, pp. 467–472.

[9] C. Fleischer and G. Hommel, "A human-exeskeleton interface utilizing electromyography," *IEEE Transactions on Robotics*, vol. 24, no. 4, pp. 872–882, 2008.

[10] J.-E. Pratt, B.-T. Krupp, C.-J. Morse, and S.-H. Collins, "The RoboKnee: An exoskeleton for enhancing strength and endurance during walking," in *Porceedings of the International Conference on Robotics and Automation*, New Orleans, USA, 2004, pp. 2430–2435.

[11] G. Aguirre-Ollinger, J.-E. Colgate, M.-A. Peshkin, and A. Groswami, "A 1-DOF assistive exoskeleton with virtual negative damping: Effects on the kinematic response of the lower limbs," in *Proceedings of International Conference on Intelligent Robots and Systems*, San Diego, CA, USA, 2007, pp. 1938–1944.

[12] ——, "Design of an active 1-DOF lower-limb exoskeleton with inertia compensation," *International Journal of Robotics Research*, 2010.

[13] W.-B. Dunbar, R.-A. de Callafon, and J.-B. Kosmatka, "Coulomb and viscous friction fault detection with application to a pneumatic actuator," in *Proceedings of IEEE/ASME International Conference on Advanced Intelligent Mechatronics*, vol. 2, Como, Italy, 2001, pp. 1239–1244.

[14] D.-A. Winter, *Biomechanics and motor control of human movement*, 4^{th} ed., Wiley, Ed. John Wiley & Sons, 2009.

[15] J. Swevers, C. Ganseman, D. Bilgin, J. De Schutter, and H. Van Brussel, "Optimal robot excitation and identification," *IEEE Transactions on Robotics and Automation*, vol. 13, no. 5, pp. 730–740, 1997.

[16] A. Teel, "Global stabilization and restricted tracking for multiple integrators with bounded controls," *Systems & Control Letters*, vol. 18, no. 3, pp. 165–171, 1992.

[17] H. Sussmann, E. Sontag, and Y. Yang, "A general result on the stabilization of linear systems using bounded controls," *IEEE Transactions on Automatic Control*, vol. 39, no. 12, pp. 2411–2425, 1994.

[18] E. N. Johnson and S. K. Kannan, "Nested saturation with guaranteed real poles," in *American Control Conference*, 2003.

[19] N. Marchand and A. Hably, "Global stabilization of multiple integrators with bounded controls," *Automatica*, vol. 41, no. 12, pp. 2147–2152, 2005.

[20] N. Marchand, "Further results on global stabilization for multiple integrators with bounded controls," in *IEEE Conference on Decision and Control, CDC'2003*, vol. 5, Hawai, USA, 2003, pp. 4440–4444.

[21] J. Guerrero-Castellanos, A. Hably, N. Marchand, and S. Lesecq, "Bounded attitude stabilization: Application on four rotor helicopter," in *Proceedings of the 2007 IEEE Int. Conf. on Robotics and Automation*, Roma, Italy, 2007, pp. 730–735.

[22] A. Zavala-Rio and V. Santibañez, "A natural staurating extension of the PD-with-desired-gravity-compensation control law for robot manipulators with bounded inputs," *IEEE Transactions on Robotics*, vol. 23, no. 2, pp. 386–391, 2007.

[23] E. Aguiñaga-Ruiz, A. Zavala-Rio, V. Santibañez, and F. Reyes, "Global trajectory tracking through static feedback for robot manipulators with bounded inputs," *IEEE Transactions on Control Systems Technology*, vol. 17, no. 4, pp. 934–944, 2009.